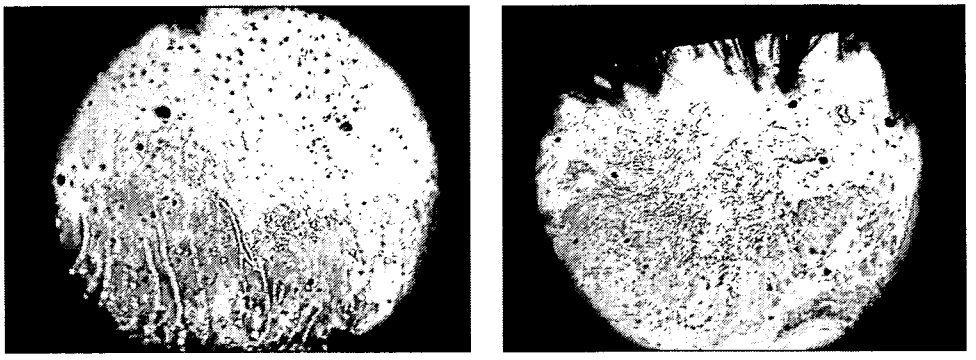

FIGURE. Representative DR-1 tear interference images from the Sjögren syndrome (SS) aqueous tear deficiency (ATD) and the non-SS ATD groups. (Left) Representative DR-1 image from a 65-year-old Asian woman in the SS ATD group. Tear evaporation rates were 5.7 (10^{-7} g/cm^2 per second), the Yokoi DR-1 grading was 4, and the range of lipid layer thickness estimated from the DR-1 tear interference image was 40 to 240 nm. Fluorescein and rose bengal scores were 6 and 5, respectively. The tear break-up time (BUT) was one second, the Schirmer I test value was 3 mm, and meibomian gland expressibility grading was 3. (Right) Representative DR-1 image from a 73-year-old Asian woman in the non-SS ATD group. Tear evaporation rates were 1.1 (10^{-7} g/cm^2 per second), the Yokoi DR-1 grading was 4, and the range of lipid layer thickness estimated from the DR-1 tear interference image was 120 to 220 nm. Fluorescein and rose bengal scores were 5 and 4, respectively. The tear BUT was four seconds, the Schirmer I test value was 2 mm, and meibomian gland expressibility grading was 2.

Japanese diagnostic criteria of dry eye was used for the diagnosis of dry eye, and Schirmer I test results of 5 mm or less were regarded as ATD.[16] Both eyes of all subjects underwent measurement. Only those eyes with Schirmer I test results of 5 mm or less were included as ATD eyes in this study. None of the subjects had any evidence of ocular infection, none wore contact lenses, none had undergone punctal occlusion, and none had blepharospasm, conjunctivochalasis, or abnormal blinking. Severe dry eye states, such as Stevens-Johnson syndrome or ocular pemphigoid, and cases with allergic conjunctivitis were excluded from the study.

• TEAR EVAPORIMETER SET UP: Tear evaporation rates from the ocular surface were measured noninvasively using our recently reported device.[11] Briefly, the evaporimeter consisted of an eye cup in the form of a ventilated chamber having a volume of 20 cm^3 that tightly covered the eye; air, which was supplied into the cup as a tear evaporation carrier by an air compressor at a constant flow rate (150 ml/minute), and a quartz crystal sensor (9 MHz A-T cut quartz crystal 8 mm in diameter and 0.2 mm in thickness), known as the microbalance, which is highly sensitive to humidity. The frequency of the sensor shifts in response to changes in humidity. Evaporation rates were measured by calculating the difference between the water content of the air entering and exiting the cup. The data sampling rate was four times per second. Real-time changes in the frequency data appeared on the display of a personal computer, synchronous with this sampling rate. For the measurement, the same eye cup was used as in the previous study to fix the condition.[11]

• EXAMINATIONS OF TEARS, THE OCULAR SURFACE, AND MEIBOMIAN GLANDS: Tear lipid layer interferometry was performed noninvasively after tear evaporimetry using the DR-1 camera system[12] (Kowa, Nagoya, Japan) before any invasive examination. DR-1 tear interference images were recorded using a digital photo printer, and the evaluation of tear interference images was carried out using the Yokoi semiquantitative dry eye severity grading system as reported previously: grade 1, somewhat gray color, uniform distribution; grade 2, somewhat gray color, nonuniform distribution; grade 3, a few colors, nonuniform distribution; grade 4, many colors, nonuniform distribution; grade 5, corneal surface partially exposed. In their report, normal control eyes were classified into grades 1 and 2 and dry eyes were classified into grades 2, 3, 4, and 5.[12,13] For the most recent data from 16 eyes of eight patients (six eyes of three SS patients, and 10 eyes of five non-SS patients), DR-1 images were acquired using the uncompressed high-quality image capturing system,[17,18] and tear lipid layer thickness was quantified using a computer-synthesized interference color chart system in the representative cases.[14]

Examination of the ocular surface was performed identically as in a previous report using the new tear evaporimetry.[11] Briefly, the ocular surface was examined by the double-staining method with 2 μl preservative-free solution consisting of 1% fluorescein and 1% rose Bengal dye. Fluorescein and rose bengal staining scores (minimum, zero; maximum, nine) and tear break-up times (BUT) were recorded.[19,20] The Schirmer I test also was performed. To assess meibomian gland expressibility, the Shimazaki grading system was used.[9] Digital pressure was applied on the lower tarsus, and the degree of ease of expression of

TABLE. Comparison of Tear Evaporimetry, Tear Interferometry, and Ocular Signs between the Sjögren Syndrome Aqueous Tear Deficiency and non-Sjögren Syndrome Aqueous Tear Deficiency Groups

	Tear Evaporation Rates (10^{-7} g/cm^2 per second)	DR-1 Grading (1–5)	Fluorescein Staining Score (0–9)	Rose Bengal Staining Score (0–9)	Tear BUT (sec)	Schirmer I Test Value (mm)	Meibomian Gland Expressibility (0–3)
SS ATD (n = 24)	5.9 ± 3.5	3.9 ± 1.2	3.0 ± 2.4	3.7 ± 2.6	2.6 ± 1.7	2.5 ± 2.0	2.2 ± 0.4
Non-SS ATD (n = 21)	2.9 ± 1.8	2.9 ± 1.1	0.9 ± 1.6	1.9 ± 2.5	3.1 ± 2.6	2.0 ± 2.0	1.0 ± 1.3
P value	.0009	.03	.002	.01	.95	.3	.04

ATD = aqueous tear deficiency; BUT = tear break-up time; SS = Sjögren syndrome.

meibomian secretions was evaluated semiquantitatively as follows: grade 0, clear fluid easily expressed; grade 1, cloudy fluid expressed with mild pressure; grade 2, cloudy fluid expressed with more than moderate pressure; and grade 3, fluid cannot be expressed even with strong pressure.

• STATISTICAL ANALYSIS: All data are shown as the mean ± standard deviation. The Mann–Whitney *U* test was applied to the comparison between SS ATD and non-SS ATD groups in the examinations. A level of $P < .05$ was accepted as statistically significant. Graphpad Instat software version 3.0 (Graphpad Software, Inc, San Diego, California, USA) was used for statistical analysis.

RESULTS

• TEAR EVAPORATION RATES AND TEAR LIPID LAYER INTERFEROMETRY: Tear evaporation rates were 5.9 ± 3.5 (10^{-7} g/cm^2 per second) in the SS ATD group, which was significantly higher than the non-SS ATD group, 2.9 ± 1.8 (10^{-7} g/cm^2 per second; Table; $P = .0009$). The SS ATD group revealed DR-1 severity grading of 3.9 ± 1.2 (Figure, Left), which was significantly higher than DR-1 grading of the non-SS ATD group, 2.9 ± 1.1 (Figure, Right; $P = .03$).

• COMPARISON OF OCULAR SIGNS IN SS ATD AND NON-SS ATD GROUPS: The corneal fluorescein mean score was 3.0 ± 2.4 in the SS ATD group, which was significantly higher than the non-SS ATD group, 0.9 ± 1.6 (Table; $P = .002$). Similarly, the mean rose bengal score was 3.7 ± 2.6 in the SS ATD group, which was also significantly higher than in the non-SS ATD group, 1.9 ± 2.5 ($P = .01$). However, tear BUT (2.6 ± 1.7 seconds in the SS ATD group and 3.1 ± 2.6 seconds in the non-SS ATD group; $P = .95$) and Schirmer I test values (2.5 ± 2.0 mm in the SS ATD group and 2.0 ± 2.0 mm in the non-SS ATD group; $P = .3$) were not significantly different. Meibomian gland expressibility grading was 2.2 ± 0.4 in the SS ATD group, which was significantly higher than the non-SS ATD group, 1.0 ± 1.3 ($P = .04$).

DISCUSSION

IN THIS ARTICLE, WE REPORT TEAR EVAPORATION RATES IN SS ATD and the non-SS ATD groups. Tear evaporation rates were significantly higher in the SS ATD group compared with the non-SS ATD group, along with worse DR-1 severity grading, vital staining scores of the ocular surface, and meibomian gland expressibility grading (Table).

In the current study, tear evaporation rates were 5.9 ± 3.5 (10^{-7} g/cm^2 per second) and 2.9 ± 1.8 (10^{-7} g/cm^2 per second) in the SS ATD and the non-SS ATD groups, respectively. These results could be compared with those from our previous report about MGD (5.8 ± 2.7 [10^{-7} g/cm^2 per second]) and normal subjects (4.1 ± 1.4 [10^{-7} g/cm^2 per second]) using exactly the same evaporimeter setup.[11] Tear evaporation rates in the SS ATD group were close to those of the MGD subjects and were significantly higher than the normal subjects. Tear evaporation rates in the non-SS ATD group were significantly lower than normal subjects. As mentioned, tear evaporation rates, which were measured by our new ventilated chamber system,[11] in dry eyes with SS ATD, in dry eyes without SS ATD (this study), and also in eyes with MGD[11] showed similar trends to those reported in previous studies by our group using the closed chamber tear evaporimeter system.[9,10] However, as we pointed out in our previous report,[11] tear evaporation rates in ATD have been inconsistent in the literature. Rolando and associates and Mathers and associates, who used the modified closed chamber system, reported increased tear evaporation rates in ATD compared with normal subjects.[6,7] On the contrary, decreased tear evaporation rates in ATD have been reported by our group using the closed chamber tear evaporimeter system[10] and by Hamano and associates compared with normal subjects.[8] Because of these inconsistencies, we decided to examine the lipid layer status simultaneously with tear evaporimetry.

The difference in tear evaporation rates in ATD dry eye states could be explained by the observation of surface lipid layer status, which has been known to affect tear evaporation.[4,21] This lipid layer condition had been assumed by the observation of meibomian gland secretion at the lid margin.[9,13,22,23] However in this report, we observed the

tear surface lipid layer directly by using the DR-1 tear interference camera.

DR-1 severity grading in the present study was significantly higher in the SS ATD group (3.9 ± 1.2) compared with the non-SS ATD group (2.9 ± 1.1). DR-1 data showed increased dry eye severity grading in the SS ATD and the non-SS ATD groups compared with the previously reported data from normal subjects (1.5 ± 0.5).[12]

The representative DR-1 images from the SS ATD and the non-SS ATD groups are shown in the Figure, which revealed similar DR-1 grading, vital staining scores, tear BUT, and Schirmer I test values. However, tear evaporation rates were higher in the SS ATD group compared with the non-SS ATD group. Meibomian gland expressibility was worse and distribution of precorneal tear lipid was more uneven (lipid layer thickness range, 40 to 240 nm) in the SS ATD group compared with the non-SS ATD group in these representative cases. Such an uneven distribution and deficient lipid level on the upper cornea (Figure, Left) may result in higher tear evaporation rates in the SS ATD group compared with the non-SS ATD group.

However, it is also evident from the lipid layer thickness data that patients with non-SS ATD with better meibomian gland expressibility have a relatively more even distribution of lipid layer thickness over the cornea with a smaller range of thickness variation (Figure, Right; 120 to 220 nm). The non-SS ATD group had lower tear evaporation rates compared with the SS ATD group. Therefore, tear evaporation measurement when carried out with DR-1 may explain the difference in clinical findings.

For the evaluation of DR-1 tear interference images, the Yokoi severity grading system was used.[12,13] When we began the present study, a lipid layer thickness quantification system was not yet available. If we could have applied this system to all DR-1 images, the correlation between tear lipid layer thickness and tear evaporation might have been obtained more clearly. However, as we reported recently, the Yokoi severity grading system may be interpreted roughly as lipid layer thickness information as follows: grades 1 and 2, lipid layer thickness approximately 10 to 92.5 nm in dark to bright brownish-gray interference color; grade 3, lipid layer thickness from 100 to 185 nm in brown interference color; grade 4, lipid layer thickness from 190 nm to 370 nm in colorful interference images; and grade 5, no movement of interference image, indicating no lipid presence, lipid layer thickness approximately 0 nm.[24] Thus, we could judge tear lipid layer thickness condition from the Yokoi grading system. Furthermore, for the most recent data, a lipid layer thickness quantification system was applied.[14,24,25]

As shown in the Figure, analysis of distribution of precorneal tear lipid would be important, and the development of its index for the comparison of the data would be highly expected in future studies. Furthermore, in the future, tear evaporimtery of the other dry eye subtypes such as dry eyes with only decreased tear film BUT would be highly anticipated.[26]

In conclusion, we applied the new tear evaporimeter system to ATD dry eye states. Meibomian gland expressibility and precorneal lipid layer conditions examined by tear interferometry may explain the resultant tear evaporation rates in ATD dry eyes. This method can contribute to further understanding in the pathogenic mechanism of dry eyes and may give us clues for better treatment of dry eye patients.[27]

THIS STUDY WAS SUPPORTED BY GRANT NO.18070501 FROM THE JAPANESE MINISTRY OF HEALTH, LABOUR, AND WELFARE, Tokyo, Japan; Japanese patent application 2003-032898 (Drs Goto, Endo, and Tsuboto); and Japanese patent application 2003-032899 (Drs Endo and Tsuboto) for the evaporimeter set-up described herein as a "Tear Secretion Quantify Examination System." Drs Endo, Tsuboto, and Goto also have filed a US patent application on the method described herein and its clinical applications as "Tear Secretion Quantify Examination System." Drs Goto, Matsumoto, and Kamoi contributed equally to the work and therefore should be considered equivalent first authors. Involved in design of study (E.G., Y.M., M.K., R.I.); conduct of study (E.G., Y.M., M.K., K.E.); collection and analysis of the data (E.G., Y.M., K.E., R.I., M.K., T.K., K.T.); and approval of the manuscript (E.G., M.D., K.T.). The present research followed the tenets of the Declaration of Helsinki based on a protocol approved by the Institutional Review Board committee of Tokyo Dental College. Informed consent was obtained from all the subjects after explanation of the nature and possible consequences of the study. This clinical trial was registered to Japan Pharmaceutical Information Center (Tokyo, Japan, JapacCTI-060313).

The authors would like to thank Mr Hirayuki Sato, Analytical Research Center, KAO Corporation, Tochigi, Japan, Mr Atsushi Suzuki, Health Care Products Research Laboratories No. 2, KAO Corporation, Tokyo, Japan, and Naoshi Shinozaki, Executive Director, Cornea Center & Eye Bank, Tokyo Dental College, Chiba, Japan, for their instruction of the principles of the interference phenomena.

REFERENCES

1. Lemp MA. Report of the National Eye Institute/Industry Workshop on Clinical Trials in Dry Eyes. CLAO J 1995;21: 221–232.
2. Pflugfelder SC, Tseng SCG, Sanabria O, et al. Evaluation of subjective assessments and objective diagnostic tests for diagnosing tear-film disorders known to cause ocular irritation. Cornea 1998;17:38–56.
3. Driver PJ, Lemp MA. Meibomian gland dysfunction. Surv Ophthalmol 1996;40:343–367.
4. Tiffany JM. The lipid secretion of the meibomian glands. Adv Lipid Res 1987;22:1–62.
5. Mathers WD, Daley TE. Tear flow and evaporation in patients with and without dry eye. Ophthalmology 1996;103: 664–669.
6. Mathers WD, Binarao G, Petroll M. Ocular water evaporation and the dry eye. A new measuring device. Cornea 1993;12:335–340.
7. Rolando M, Refojo MF, Kenyon KR. Increased tear evaporation in eyes with keratoconjunctivitis sicca. Arch Ophthalmol 1983;101:557–558.

8. Hamano H, Hori M, Mitsunaga S. Application of an evaporimeter to the field of ophthalmology. J Jpn Contact Lens Soc 1980;22:101–107.
9. Shimazaki J, Goto E, Ono M, Shimmura S, Tsubota K. Meibomian gland dysfunction in patients with Sjögren syndrome. Ophthalmology 1998;105:1485–1488.
10. Tsubota K, Yamada M. Tear evaporation from the ocular surface. Invest Ophthalmol Vis Sci 1992;33:2942–2950.
11. Goto E, Endo K, Suzuki A, Fujikura Y, Matsumoto Y, Tsubota K. Tear evaporation dynamics in normal subjects and subjects with obstructive meibomian gland dysfunction. Invest Ophthalmol Vis Sci 2003;44:533–539.
12. Yokoi N, Takehisa Y, Kinoshita S. Correlation of tear lipid layer interference patterns with the diagnosis and severity of dry eye. Am J Ophthalmol 1996;122:818–824.
13. Yokoi N, Mossa F, Tiffany JM, Bron AJ. Assessment of meibomian gland function in dry eye using meibometry. Arch Ophthalmol 1999;117:723–729.
14. Goto E, Dogru M, Kojima T, Tsubota K. Computer-synthesis of an interference color chart of human tear lipid layer, by a colorimetric approach. Invest Ophthalmol Vis Sci 2003;44:4693–4697.
15. Fox RI, Saito I. Criteria for diagnosis of Sjögren's syndrome. Rheum Dis Clin North Am 1994;20:391–407.
16. Danjo Y. Diagnostic usefulness and cutoff value of Schirmer's I test in the Japanese diagnostic criteria of dry eye. Graefes Arch Clin Exp Ophthalmol 1997;235:761–766.
17. Goto E, Tseng SC. Differentiation of lipid tear deficiency dry eye by kinetic analysis of tear interference images. Arch Ophthalmol 2003;121:173–180.
18. Goto E, Tseng SC. Kinetic analysis of tear interference images in aqueous tear deficiency dry eye before and after punctal occlusion. Invest Ophthalmol Vis Sci 2003;44:1897–1905.
19. Toda I, Tsubota K. Practical double vital staining for ocular surface evaluation. Cornea 1993;12:366–367.
20. van Bijsterveld OP. Diagnostic tests in the Sicca syndrome. Arch Ophthalmol 1969;82:10–14.
21. Mishima S, Maurice DM. The oily layer of the tear film and evaporation from the corneal surface. Exp Eye Res 1961;1:39–45.
22. Shimazaki J, Sakata M, Tsubota K. Ocular surface changes and discomfort in patients with meibomian gland dysfunction. Arch Ophthalmol 1995;113:1266–1270.
23. Mathers WD. Ocular evaporation in meibomian gland dysfunction and dry eye. Ophthalmology 1993;100:347–351.
24. Goto E. Quantification of tear interference image: tear fluid surface nanotechnology. Cornea 2004;23:S20–S24.
25. King-Smith PE, Fink BA, Fogt N. Three interferometric methods for measuring the thickness of layers of the tear film. Optom Vis Sci 1999;76:19–32.
26. Toda I, Shimazaki J, Tsubota K. Dry eye with only decreased tear break-up time is sometimes associated with allergic conjunctivitis. Ophthalmology 1995;102:302–309.
27. Goto E, Dogru M, Fukagawa K, et al. Successful tear lipid layer treatment for refractory dry eye in office workers by low-dose lipid application on the full-length eyelid margin. Am J Ophthalmol 2006;142:264–270.

Biosketch

Eiki Goto, MD, is an Associate Professor of the Department of Ophthalmology, School of Dental Medicine, Tsurumi University, Japan. Dr Goto received his medical degree from the School of Medicine, Keio University, Japan and did his Research Fellow at Bascom Palmer Eye Institute, University of Miami, Miami, Florida. Dr Goto is affiliated with Japanese Cornea Society and Tear Film and Ocular Surface Society. Dr Goto's primary research interests are dry eye, tear interferometry, and lipid layer treatment.

Research Paper

Journal of Vascular Research

J Vasc Res 2007;44:138–148
DOI: 10.1159/000098520

Received: February 16, 2006
Accepted after revision: November 19, 2006
Published online: January 11, 2007

Functional Analysis of an Established Mouse Vascular Endothelial Cell Line

Tatsuaki Nishiyama[a, b] Kenji Mishima[a] Fumio Ide[a] Koichi Yamada[a]
Kumi Obara[a] Aki Sato[a] Noriko Hitosugi[a] Hiroko Inoue[a] Kazuo Tsubota[b, c]
Ichiro Saito[a, b]

[a]Department of Pathology, Tsurumi University School of Dental Medicine, Yokohama;
[b]Sjögren's Syndrome Project, Shinanomachi Research Park, and [c]Department of Ophthalmology,
Keio University School of Medicine, Tokyo, Japan

Key Words
Cellular binding · Endothelial cell line · p53-deficient mice · Tube formation

Abstract
Background: In vitro studies using cell lines are useful for the understanding of cellular mechanisms. The purpose of our study is to develop a new immortalized aortic vascular endothelial cell (EC) line that retains endothelial characteristics and can facilitate the study of ECs. ***Methods:*** A mouse aortic vascular EC line (MAEC) was established from p53-deficient mouse aorta and cultured for over 100 passages. The expression of endothelial markers was assessed, and the function of this cell line was analyzed by tube formation and binding assays. ***Results:*** MAEC retained many endothelial properties such as cobblestone appearance, contact-inhibited growth, active uptake of acetylated low-density lipoprotein, existence of Weibel-Palade bodies and several EC markers. MAECs exhibited tube formation activity both in vitro and in vivo. Furthermore, crucially, tumor necrosis factor α, an inflammatory cytokine, promoted lymphocyte adhesion to MAECs, suggesting that MAECs may facilitate the study of atherosclerosis and local inflammatory reactions in vitro. ***Conclusion:*** We describe the morphological and cell biological characteristics of MAEC, providing strong evidence that it retained endothelial properties. This novel cell line can be a useful tool for studying the biology of ECs.

This work was partially supported by grants-in-aid for scientific research from the Ministry of Education, Culture, Sports, Science and Technology of Japan.

Introduction

Endothelial cells (ECs) line the inner surface of blood and lymphatic vessels and play critical roles in vasculogenesis, angiogenesis, the development and remodeling of the vasculature, vascular permeability and circulation [1]. In vitro studies using EC lines or primary ECs are highly useful to understand the mechanisms of the results gained from in vivo analyses. The development of techniques for the isolation and growth of ECs in vitro [2] has resulted in a dramatic increase in our understanding of endothelial function. For human studies, a number of in vitro experimental EC models have been developed using human umbilical vein ECs (HUVECs) [3, 4]. For

KARGER

Fax +41 61 306 12 34
E-Mail karger@karger.ch
www.karger.com

1018–1172/07/0442–0138$23.50/0

Accessible online at:
www.karger.com/jvr

Dr. Ichiro Saito
Department of Pathology, Tsurumi University School of Dental Medicine
2-1-3 Tsurumi, Tsurumi-ku
Yokohama, 230-8501 (Japan)
Tel. +81 45 580 8360, Fax +81 45 572 2888, E-Mail saito-i@tsurumi-u.ac.jp

mouse studies, ECs have been isolated from murine lung [5], lymph nodes [6], and brain [7]. However, the isolation of primary ECs from mouse organs is both time consuming and costly, and the ECs of some organs can only be passaged two or three times before significant senescence occurs [8]. These problems can be overcome by the use of immortalized cell lines because they show stable proliferation and clonality. Numerous attempts have been made by researchers to establish mouse EC lines. Although several mouse and rat EC lines have been established, the immortalization resulted in phenotypic changes, such as a decrease in surface antigens [9] and tube-forming activity [10], and less responsiveness to cytokines [11]. Considering these reports, immortalized EC lines retaining the differentiated characteristics of the original tissues are useful materials for the study of EC proliferation, differentiation, and metabolism. In addition, no aortic EC lines have been described previously.

Gene transfer of simian virus 40 (SV40) T antigen is frequently used for cell immortalization, and some cell lines immortalized by SV40 T antigen-encoding transgenes have proven useful in studies on the regulation of gene expression [12]. However, present disadvantages of SV40 vectors are the possible risks related to random integration of the viral genome into the host genome. On the other hand, p53-deficient mice used in this study have only one mutation in the p53 gene. In addition, the DNA content of homozygous cells, which remained in the diploid range, had no chromosomal aberrations [13].

The p53 gene is thought to regulate the process of the cell cycle to induce cell arrest and cell death in normal cells, and the deletion of this gene has been used for cell immortalization. Some cell lines established from p53-deficient mice have been reported, including an osteoblast cell line [14], a pulmonary alveolar type II cell line [15], a prostatic cell line [16], a cerebellar cell line [17], and an astrocyte cell line [18]. Furthermore, an established colon epithelial line did not form colonies in soft agar and was non-tumorigenic in SCID mice [19]. These reports indicate that p53-deficiency is sufficient for immortalization of cells and that the loss of p53 itself does not cause the acquisition of malignant properties. Thus p53-deficient mice are useful for establishing cell lines.

The purpose of our present study is to develop a mouse aortic vascular EC line (MAEC) derived from p53-deficient mouse aorta, and to demonstrate the utility of this cell line in functional assays. We here describe the cell-biological characteristics and function of the MAEC, thus enhancing our understanding of the role of ECs.

Methods

Mice

All animal experimental protocols were approved by the Tsurumi University Ethics Committee. The p53-deficient mice were provided by Dr. Shinichi Aizawa (RIKEN, Tsukuba, Japan). Characterization of the p53-deficient mice has been reported in detail previously [13].

Establishment of Cell Lines from p53-Deficient Mice and Cell Culture

Vascular ECs were prepared as described previously [20] with some modifications. Aorta was harvested from an 8-week-old, female, p53-deficient mouse, minced into 1-mm^2 pieces, washed in Hanks' balanced salt solution without Ca^{2+} and Mg^{2+} (Sigma, St. Louis, Mo., USA), and incubated in a 60-mm dish containing 0.76 mg/ml EDTA, 4.9 mg/ml L-ascorbic acid, and 4.9 mg/ml glutathione at 37°C for 15 min. The minced tissue was washed with soybean trypsin inhibitor (Sigma)/Dulbecco's modified Eagle's medium (DMEM; Sigma) and digested in a mixture of collagenase (type I: 750 U/ml, Wako, Osaka, Japan) and hyaluronidase (type IV: 500 U/ml, Sigma) dissolved in DMEM/F12 (Sigma) containing 10% fetal bovine serum (FBS; BioWhittaker, Walkersville, Md., USA). The first digest suspension was passed through a sterile 100-μm nylon mesh filter, redigested for 2 h using the same digestion procedure, and then passed again through a 100-μm nylon mesh filter. The growth medium employed in this study was M199 medium (Sigma) with 5 ng/ml of recombinant vascular endothelial growth factor (VEGF; Sigma), Hepes (Invitrogen, Carlsbad, Calif., USA), heparin sodium (Shimizu, Shizuoka, Japan) and 5% FBS. HUVECs were cultured in EGM-2 SingleQuots (Cambrex Bio Science Walkersville, Walkersville, Md., USA) and mouse fibroblast cell line (NIH3T3) was cultured in DMEM with 10% FBS. Cells were cultured in humidified incubators at 37°C in an atmosphere of 5% CO_2 and 95% air, and the medium was exchanged every 2–3 days.

DiI-Ac-LDL Uptake Study

MAECs, HUVECs and NIH3T3 cells grown in dishes were incubated for 4 h at 37°C with complete medium containing 10 μg/ml of DiI-Ac-LDL (Biogenesis, Poole, UK). After removal of the medium, the cells were washed three times with PBS and visualized using fluorescent microscopy (Olympus, Melville, N.Y., USA) or analyzed by flow cytometry (Becton Dickinson, Franklin Lakes, N.J., USA).

Flow-Cytometric Analysis

The cultured MAECs were dissociated by treatment with cell dissociation solution (Sigma), harvested by centrifugation and stained with fluorescein isothiocyanate (FITC) conjugated *Griffonia simplicifolia* isolectin B4 (GSLI-B4; Vector Laboratories, Peterborough, UK) and then analyzed by flow cytometry. The cells that took up DiI-Ac-LDL as described above were also monitored and sorted by flow cytometry. Expression of vascular cell adhesion molecule-1 (VCAM-1) on MAECs and very late antigen-4 (VLA-4) on a murine myelomonocytic leukemia cell line (WEHI-3B) was also analyzed by flow cytometry using anti-mouse VCAM-1 antibody, anti-mouse VLA-4 antibody and anti-rat IgG FITC conjugate (Santa Cruz Biotechnology, Santa Cruz, Calif., USA).

Ultrastructural Examination by Transmission Electron Microscopy

MAECs cultured in plastic dishes were washed in PBS and then fixed in 2.5% glutaraldehyde. After fixation in 1% osmium tetroxide, they were embedded in Epon 812. Ultrathin sections were cut by an LKB ultramicrotome, stained with uranyl acetate and lead citrate and examined using a Hitachi H-500 electron microscope.

RT-PCR Assay

Total RNA was extracted from MAECs, HUVECs, NIH3T3 and the aorta of a C57BL/6 mouse, with TRIzol reagent (Life Technologies, Rockville, Md., USA), and cDNA was prepared from RNA with 50 pmol of random hexamer and 200 U of reverse transcriptase (Invitrogen, Carlsbad, Calif., USA); 0.5 μl of a 20-μl cDNA mixture was used for PCR with 5 pmol each of forward and reverse primers and 2.5 U of Ex Taq DNA polymerase (Takara Shuzo, Kyoto, Japan). The sequences of the specific sense and antisense oligonucleotide primer pairs were as follows: VEGF receptor-2 (Flk-1), TGGCAGCACGAAACATTCT and TTGCAGGAGGTTTCCCAAAT; von Willebrand factor (vWf), TCCCAGACCATCAGCCCT and GGTAAAGGTGGGTCTGCATT; β-actin, CTCTTTGATGTCACGCACGATTTC and GTGGGCCGCTCTAGGCACCAA; intercellular adhesion molecule-2 (ICAM-2), TGCTGGAGCCTGTCTCTTCTT and TTTCCCGAACACGTGAAATG; Tie-2, TATTGAGTATGCCCCGCATG and GCTAACAATCTCCCAGAGCAA; endothelial nitric oxide synthase (eNOS) for mice, AAAGAATTGGGAAGTGGGCA and AACATTTCCTGTGCAGTCCTG, and eNOS for humans, GACGCTACGAGGAGTGGAAG and TAGGTCTTGGGGTTGTCAGG.

Samples were amplified through 35 cycles at an annealing temperature of 52°C in a PCR Thermal Cycler (Applied Biosystems, Foster City, Calif., USA).

Immunofluorescence Staining

Cytospin (Thermo Electron, Waltham, Mass., USA) preparations of MAECs were fixed in 3% (v/v) paraformaldehyde at room temperature for 15 min and blocked in DAKO Cytomation Protein Block Serum-Free Ready-to-use (DAKO, Glostrup, Denmark) for 1 h. Cells were incubated with primary antibodies, such as phycoerythrin-conjugated anti-Flk-1 monoclonal antibody (Pharmingen, San Diego, Calif., USA), anti-vascular endothelial (VE)-cadherin monoclonal antibody (Pharmingen), anti-vWf monoclonal antibody (DAKO) or ICAM-2 monoclonal antibody (Pharmingen) at 4°C overnight. As a control, isotype control (R & D Systems, Minneapolis, Minn., USA) was used as a primary antibody. After washing with cold PBS, the cells were incubated with biotin-conjugated anti-rat IgG (Chemicon, Temecula, Calif., USA) or biotin-conjugated anti-mouse IgG (Chemicon) at 4°C for 1 h. Subsequently, the cells were incubated with FITC-conjugated streptavidin (BD Biosciences, San Jose, Calif., USA) at 4°C for 1 h. Preparations were mounted in DAKO fluorescent mounting medium (DAKO) and viewed under a fluorescence microscope (TS100; Nikon, Tokyo, Japan).

Immunoblotting

The proteins obtained from MAECs and homogenized uterus were boiled in sample buffer (500 mM Tris-HCl, pH 6.8, 4% SDS, 20% glycerol, and 2% mercaptoethanol) for 5 min. Equal amounts of total protein were loaded on each lane and run on SDS-PAGE, followed by electrophoretic transfer of the proteins to polyvinylidene difluoride membrane. Membranes were first blocked with 5% skim milk for 1 h and then incubated with the mouse anti-α smooth muscle actin (α-SMA) monoclonal antibody (Research Diagnostics, Flanders, N.J., USA) or anti-tubulin monoclonal antibody (Sigma) for 1 h. After three sequential 5-min washes with washing buffer (20 mM Tris-HCl, pH 7.4, and 0.1% Tween 20), the membranes were incubated with anti-rabbit IgG or anti-mouse IgG peroxidase-conjugated secondary antibodies (Santa Cruz Biotechnology) for 1 h at room temperature and then again washed as described above. Bound protein was developed with ECL detection reagents (Amersham Biosciences, Piscataway, N.J., USA) and exposed to X-ray films for 5 s.

Transient Transfection Procedure

1.5×10^5 HUVECs and MAECs were grown on 12-well plates and transiently transfected with pcDNA™ 3.1/*myc*-His/*lacZ* (Invitrogen) using the Lipofectamine™ 2000 Transfection Reagent (Invitrogen), according to the manufacturer's protocol. For measuring transfection efficiency, transiently transfected cells were stained with a β-Gal staining set (Roche, Penzberg, Germany), and positive staining cells were counted by microscopy.

Tube Formation Assay

One hundred microliters of Matrigel (BD Biosciences) were added to 24-well culture plates (Becton Dickinson) and allowed to solidify at 37°C for 30 min. MAECs (2×10^4 cells/well) were seeded on the Matrigel and cultured in M199 medium at 37°C in a humidified atmosphere of 5% CO_2 air. After incubation for 24 h, tube formation was observed using phase-contrast microscopy and photographed.

Infection of Cells with Adenovirus

MAECs (1×10^6) were plated in 100-mm dishes, cultured overnight and incubated with 100 multiplicities of infection of recombinant adenovirus encoding *Escherichia coli* β-galactosidase (Ad-β-gal) for 1 h. Cultured medium was added and MAECs were maintained for 24 h. The recovered MAECs were used for the Matrigel plug assay described below.

In vivo Matrigel Plug Assay

Tube formation activity in vivo was assessed with the Matrigel plug assay. MAECs (2×10^6) were mixed with 0.2 ml of PBS or 0.2 ml of Matrigel and inoculated subcutaneously in 4 nude mice. Matrigel plugs were surgically removed 2 weeks after injection. Each plug was fixed with 10% (vol/vol) formaldehyde, embedded in paraffin, sectioned, and stained with hematoxylin/eosin. For β-gal staining, the removed plugs were then embedded in OCT and frozen with liquid nitrogen. Cryostat sections (5 μm) were made, and the slides were stained for β-gal activity. The slides were then fixed in PBS (pH 7.2) containing 0.25% glutaraldehyde for 10 min at 4°C and stained in 5 mM $K_4Fe(CN)_6 \cdot 3H_2O$, 5 mM $K_3Fe(CN)_6$, 0.2 mM $MgCl_2$, and 1 mg of X-Gal/ml in PBS (pH 7.2) overnight at 37°C. The sections were rinsed in PBS (pH 7.2) and stained with hematoxylin at room temperature for better visualization of the staining.

Cellular Binding Assay

MAECs (2.5×10^4) were seeded into each well of 96-well culture plates (Becton Dickinson). Confluent cultures of MAECs

were stimulated with TNFα (10 ng/ml). WEHI-3B cells (1×10^5) labeled with PKH2 (Sigma) were added to each well and incubated with MAECs for 1 h. Cells that nonspecifically bound to MAECs were removed by inverting the plates for 30 min. Wells were subsequently washed once with serum-free RPMI 1640 (Sigma), and the remaining cells were lysed with 1% Triton X-100 (Sigma). Fluorescence intensity in cell lysate was measured using an automated microplate fluorometer (Perkin Elmer, Wellesley, Mass., USA) at 490 nm. Data are expressed as the percentage of input cells bound.

Nitrate Measurement

Nitrate accumulation was determined by mixing equal volumes of cell culture medium and Griess reagent (Griess Reagent System, Promega, Madison, Wisc., USA) with absorbance at 540 nm on a microplate reader. Standard curves were constructed with known concentrations of $NaNO_2$.

Results

Isolation of Cell Lines from a p53-Deficient Mouse

Cells isolated from the p53-deficient mouse aorta were cultured with M199 medium containing 5 ng/ml recombinant mouse VEGF. Most of the growing cells were morphologically fibroblastic. The cells that showed active uptake of DiI-Ac-LDL were sorted by flow cytometry. After sorting, the collected cells continued to grow, whereas the population of fibroblastic cells diminished. In order to obtain monoclonal cell lines, the sorted cells were subjected to limiting dilution and one of the clones, No. 12, was used for further experiments. This chosen MAEC clone was serially cultured over 1 year and for more than 100 passages. The proliferation of MAECs was examined and the doubling time was 23.2 h. Active uptake of DiI-Ac-LDL of the No. 12 clone was confirmed by flow cytometry (fig. 1c) and confocal microscopy (data not shown). HUVECs clearly showed active uptake of Ac-LDL (fig. 1b), while NIH3T3 showed no uptake (fig. 1d). As active uptake of Ac-LDL is one of the well-known characteristics of ECs, these observations confirmed that MAECs retained characteristics similar to HUVECs and originated in ECs. The MAECs showed typical endothelial morphology, such as cobblestone appearance and contact-inhibited growth (fig. 1a).

Endothelial Characteristics

To investigate whether MAECs had endothelial properties, their characteristics were examined by electron microscopy. As shown in figure 2, Weibel-Palade (WP) bodies were observed in the cytoplasm [21]. WP bodies are abundant within ECs and consist of P-selectin and vWf, formerly designated factor-VIII-related antigen.

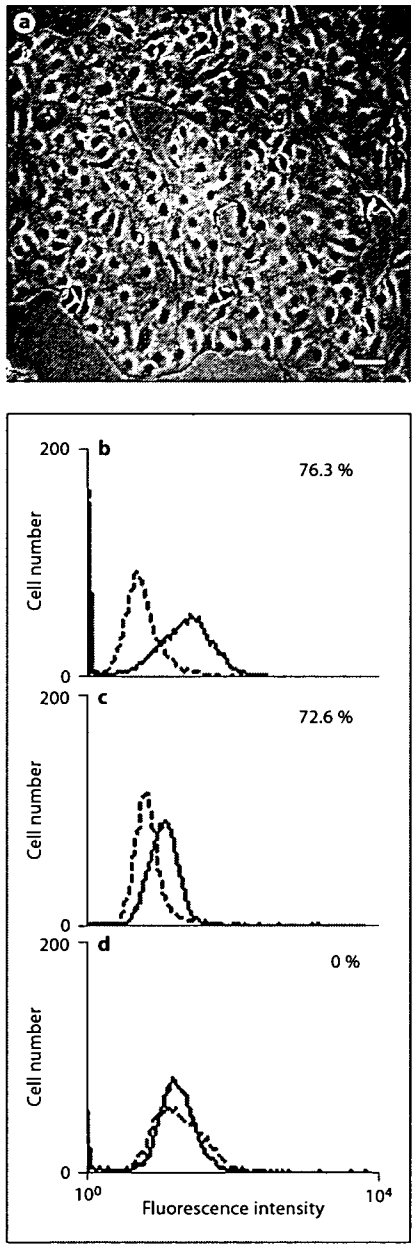

Fig. 1. Establishment and morphology of MAECs. **a** MAECs imaged under phase contrast microscopy. Cells were cultured at 37°C in M199 medium and formed cobblestone morphology with contact-inhibited growth at confluence (magnification ×400, scale bar = 50 μm). Active DiI-Ac-LDL uptake examined by flow cytometry in HUVECs as a positive control (**b**), and MAECs (**c**) and NIH3T3 as a negative control (**d**). Dotted line indicates negative controls without DiI-Ac-LDL.

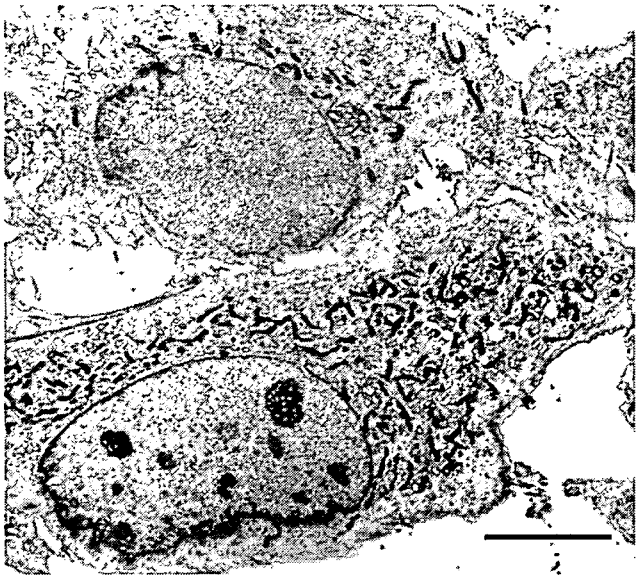

Fig. 2. Presence of WP bodies in MAECs detected by electron microscopy. Many WP bodies are recognized in the cell cytoplasm. P-selectin and vWf are stored in these cytoplasmic components, and the existence of WP bodies indicates that MAECs are ECs (magnification ×1,500, scale bar = 1 μm).

As large blood vessels, like the aorta, are surrounded by smooth muscle cells, we analyzed the possibility of smooth muscle cell contamination. α-SMA, which is a differentiated smooth muscle marker, was not revealed by immunoblotting on MAECs (fig. 3a). However, it was strongly detected in the homogenized uterus, indicating that MAECs were not contaminated by smooth muscle cells.

We next characterized their vasculogenic potential by analyzing the expression of endothelial-specific genes. MAECs were cultured at subconfluent density, and RNA was extracted for analysis of endothelial-related gene expression using RT-PCR. Expression of EC adhesion molecules such as ICAM-2 [22] and growth factor receptors such as VEGFR-2/Flk-1/KDR [23], Tie-2, and vWf [24] were detected in the aorta and MAECs but not in NIH3T3 (fig. 3b). Although the expression level was weaker than normal ECs, the expression profile of endothelial markers in MAECs was similar to that of the aorta. In order to study protein expression, MAECs were prepared by cytospin and subjected to immunofluorescence staining which demonstrated that Flk-1 (fig. 3c), VE-cadherin (fig. 3d), ICAM-2 (fig. 3e) and vWf (fig. 3f) were expressed on MAECs. These results showed that MAECs have various endothelial markers on their surfaces. Especially VE-cadherin, an endothelial-specific cadherin also known as cadherin-5, mediates cell-cell interactions through the formation of an adherence junction, which is important in maintaining vascular integrity [25]. Furthermore, GSLI-B4, which is reported to bind specifically to mouse ECs, bound to MAECs. This binding was visualized with fluorescent microscopy (fig. 3h) and assessed with flow cytometry (data not shown).

For more detailed characterization of the established cell line, transfection efficiency was determined with a liposomal transfection agent. LacZ gene was transfected to MAEC or COS-7, and the transfection efficiency was analyzed by β-gal staining. 13.5% of MAEC were stained and 58.1% of COS-7 were stained under the same conditions. These results demonstrated that MAEC can be transfected, but its efficiency is not high.

Three-Dimensional Culture of ECs in vitro and in vivo

As described above, MAECs retained the morphology and cell surface markers of ECs, and so we performed functional analysis of MAECs as ECs. One of the endothelial functions of this cell line was determined by culture on Matrigel, an extracellular matrix basement membrane that can be used to promote differentiation of ECs [26]. Most ECs rapidly organize and form tube-like structures after plating on Matrigel, and the ability to form tube-like structures on Matrigel can distinguish ECs from common contaminated cell types [5]. MAECs spontaneously reorganized tube-like structures on Matrigel after 24 h (fig. 4a), and they maintained these structures for 3 days. We studied their behavior in vivo to investigate the capacity of MAECs to participate in the process of neovascularization. We used a tumor transplantation model in athymic nude mice. The mixture of MAECs and Matrigel was subcutaneously injected into 4 mice. Athymic nude mice injected with MAECs and PBS served as a control group. Two weeks after injection, MAECs with Matrigel were removed from the mice. The sections of MAECs and Matrigel were stained with HE, and tube-like structures were microscopically detected (fig. 4b). In addition, in order to confirm whether these tube-like structures were constructed of injected MAECs and not recipient ECs, MAECs were labeled with Ad-β-gal prior to injection; thus, the expression of the *E. coli* β-gal gene was directed to the nuclear compartment. One week after injection, MAECs were removed and β-gal activity was analyzed in the frozen sections. Positive staining for β-gal was detected in the tube-like structures, therefore they were disclosed as injected MAECs (fig. 4c). These results indicate that MAECs have the capacity to form three-dimensional structures in vivo.

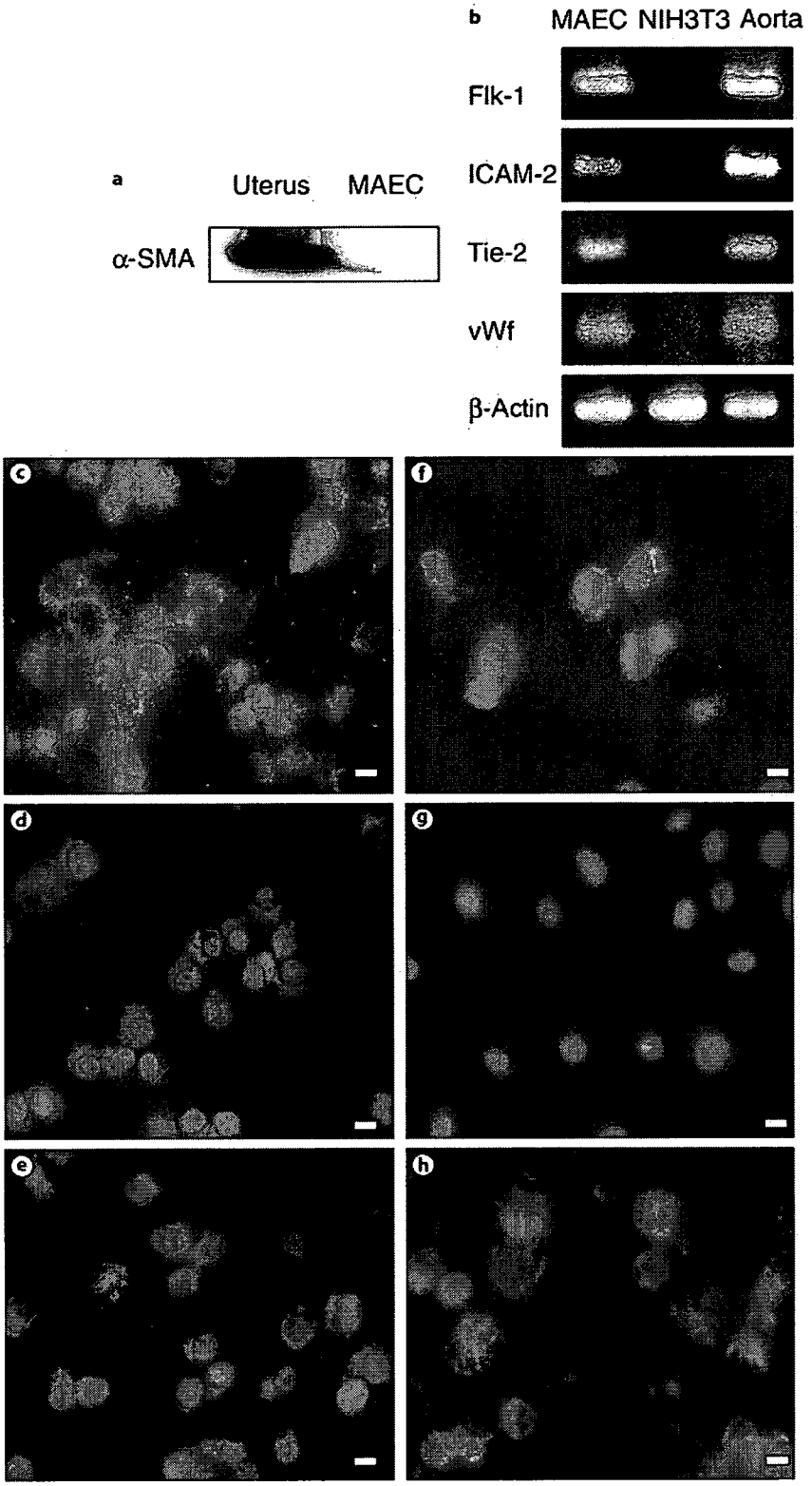

Fig. 3. Endothelial gene expression in MAECs. **a** Western blotting demonstrated that α-SMA was not expressed in MAECs. The uterus was used as a positive control. **b** RT-PCR analysis showed that Flk-1, ICAM-2, Tie-2, and vWf were expressed in MAECs but not in NIH3T3. The aorta was used as a positive control. Expression of Flk-1 (**c**), VE-cadherin (**d**), ICAM-2 (**e**), and vWf (**f**) was monitored by fluorescent microscopy. **g** Isotype control. **h** MAECs showed binding to GSLI-B4 by fluorescent microscopy (magnification ×400, scale bar = 10 μm).

Cellular Binding Activity of MAECs

To assess another endothelial function, cellular binding activity with lymphocytic cells, an in vitro cellular binding assay was performed using TNFα-stimulated MAECs and WEHI-3B cells. TNFα upregulated the expression of VCAM-1 on MAECs (fig. 5a). WEHI-3B cells expressed VLA-4, which is a ligand of VCAM-1, on their surfaces spontaneously (fig. 5b). MAECs were stimulated with 10 ng/ml TNFα and cocultured with WEHI-3B cells for 1 h. After washing, the cells which bound to the MAECs were examined with phase contrast microscopy. Figure 5c shows that cellular binding between WEHI-3B cells and TNFα-stimulated MAECs was enhanced compared with unstimulated MAECs (fig. 5d). This result indicates that TNFα-induced VCAM-1 may play a role in the binding with WEHI-3B cells via VLA-4. For quantification of the binding capacity, WEHI-3B cells labeled with PKH2 were added to MAECs and the binding of these cells was revealed by fluorescence intensity. Although 15.2% of the WEHI-3B cells bound to TNFα-stimulated MAECs, only 3.8% of WEHI-3B cells bound to unstimulated MAECs. As shown in figure 5f, the adhesion of WEHI-3B cells to TNFα-stimulated MAECs was significantly upregulated (* $p = 0.04$, stimulated vs. unstimulated MAECs, Scheffe's test).

NO Production and eNOS Expression in MAECs

Another endothelial function was evaluated: NO production and the expression of eNOS. NO accumulated in HUVEC cultured for 48 h, but little NO was detected in the MAEC culture (fig. 5g), and 100 ng/ml of VEGF did not upregulate NO production. eNOS expression was detected in MAECs by RT-PCR but not in the mouse fibroblast cell line, NIH3T3 cells (fig. 5g). This expression was weaker than that in HUVECs as well as the other endothelial markers described above. eNOS expression of MAECs may decrease during the immortalization process and it may result in low level NO production.

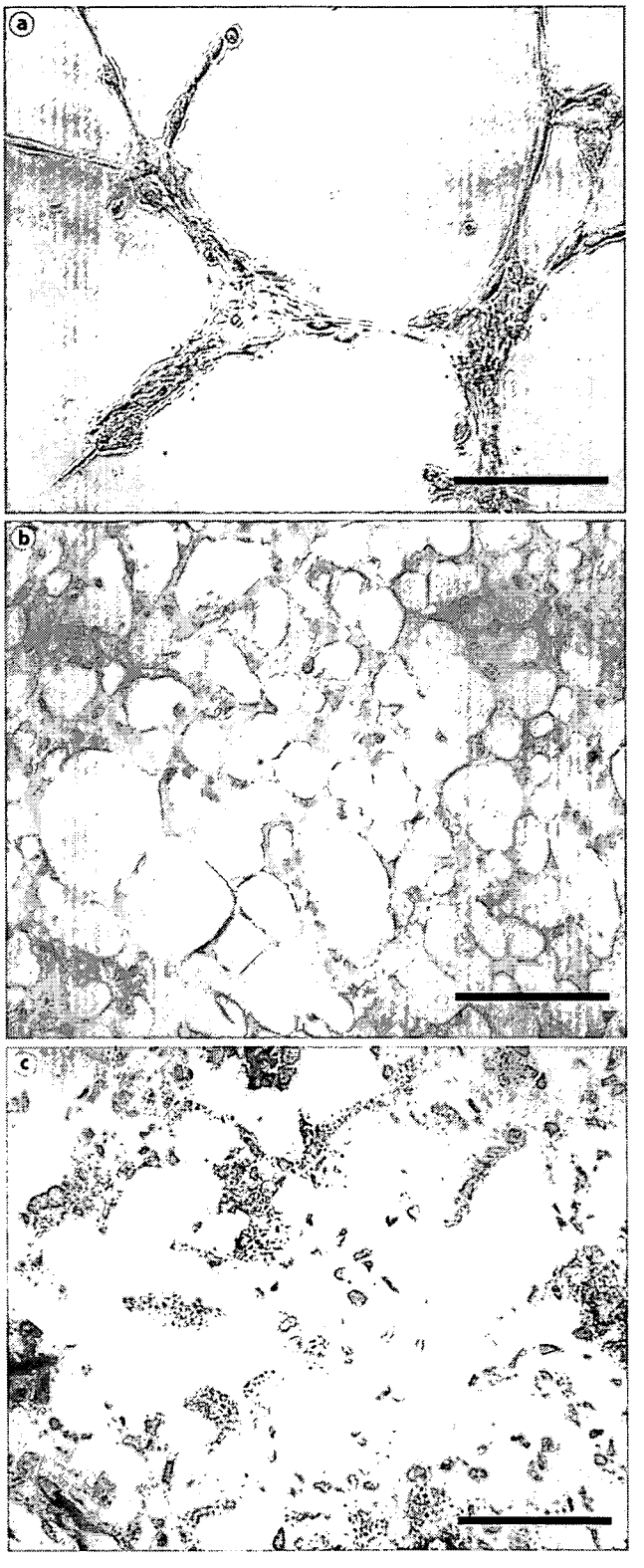

Fig. 4. Tube formation of MAECs on Matrigel and in vivo. **a** Tube formation by MAECs 24 h after seeding the cells on Matrigel (magnification ×200, scale bar = 100 μm). **b** MAECs and Matrigel were inoculated into nude mice, and removed mixtures were sectioned and analyzed by HE staining. Many tube formations were seen in the section. **c** MAECs that were transfected with Ad-β-gal were inoculated and analyzed. β-gal-labeled MAECs were seen in the sections. **b**, **c** Magnification ×400, scale bar = 50 μm.

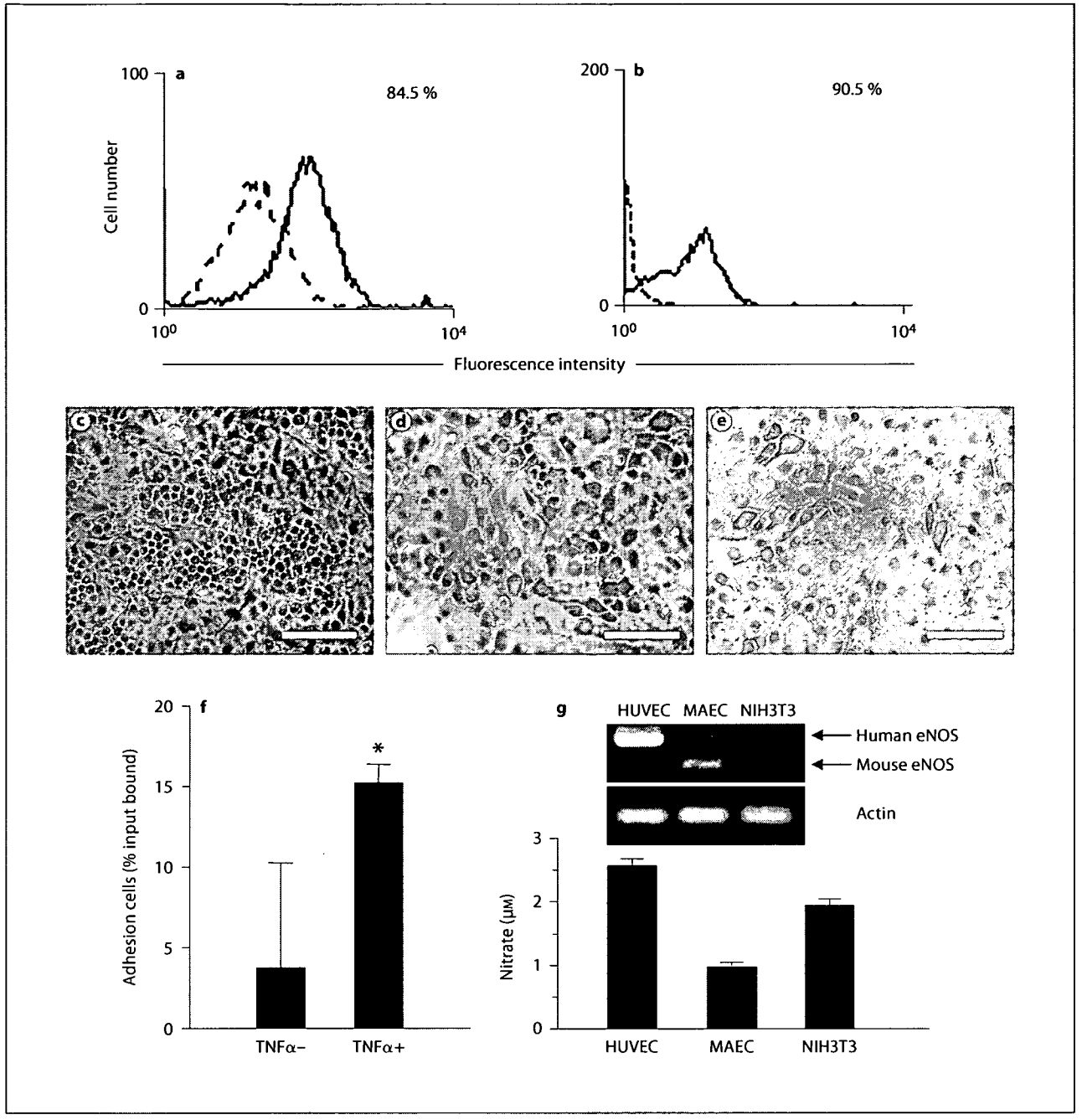

Fig. 5. a Representative histograms depict the isotype control (dotted line) and stimulated endothelial VCAM-1 expression after incubation with TNFα (10 ng/ml) for 4 h. **b** Surface expression of VLA-4 on WEHI-3B. The dotted line shows the isotype control. The data of phase contrast microscopy show cellular binding between WEHI-3B cells and TNFα-stimulated MAECs (**c**) or unstimulated MAECs (**d**). **e** The control with no WEHI-3B cells. **c–e** Magnification ×200, scale bar = 100 μm. **f** Cellular binding activity of MAECs to mononuclear cells was measured by cellular binding (* $p = 0.04$). **g** The expression of eNOS by RT-PCR and nitrate production in MAEC. **f, g** The results are representative of several experiments.

Discussion

In order to understand the mechanism of events shown in in vivo analysis, it is important to reconstruct them in in vitro experiments. HUVECs contributed to these in vitro analyses for human EC biology. For in vivo experiments using mice, some mouse EC lines were previously reported [27–30], and these cell lines each had endothelial-like characteristics and were useful to some degree. Although Su et al. [30] showed tube formation of their cell line on Matrigel, no other EC functions were reported in their studies. A cell line that retains as many similar functions to normal ECs as possible is required for various in vitro analyses. In our present study, we assessed the characteristics and functions of the newly established EC line, MAECs. MAECs exhibited typical and basic criteria for the identification of ECs [31], e.g. cobblestone appearance, contact-inhibited growth and active uptake of DiI-Ac-LDL. In addition to these characteristics, electron-microscopic analysis showed the existence of WP bodies, which are the endothelial-specific storage organelle for the regulation of vWf secretion. These results indicate MAECs are an EC line.

The differentiation of the EC lineage was assessed in a previous study [32]. Flk-1 is the early marker for endothelial progenitors and is expressed in isolated mesodermal cells that give rise to ECs and in hematopoietic cell progenitors, termed hemangioblasts. In addition, Flk-1 is expressed in various differentiation stages of ECs and is essential for EC differentiation [32–34]. Hirashima et al. [32] showed that Flk-1+ EC progenitor cells start to express VE-cadherin and CD31 and differentiate to ECs in vasculogenesis [32, 34]. Tie-2 is a receptor for both angiopoietin-1 and angiopoietin-2 and is particularly expressed in ECs [35] but also in the late stage of vascular morphogenesis [34]. Furthermore, vWf is a marker for differentiated ECs [10, 28]. We detected Flk-1 and other endothelial markers such as VE-cadherin, ICAM-2, vWf, and Tie-2 on MAECs. Therefore, these results showed that MAECs have differentiated characteristics of ECs.

Here, we investigated three functional analyses for MAECs; tube formation assay, cellular binding assay, and NO production to examine if the cell line was suitable for vascular research. The tube formation of ECs on Matrigel has been used as an in vitro angiogenesis assay [3, 4]. MAECs showed tube formation activity on Matrigel suggesting that they can be used for angiogenesis studies. MAECs also exhibited tube formation in nude mice with Matrigel, indicating that they retain the potential to organize a vascular network in vivo and that they can be used for wider applications in endothelial or vascular research. However, we have to consider that MAECs may not be the ideal model for studying angiogenesis under stressful conditions such as irradiation being imposed on the cells, because of its deficiency in p53 which plays an important role in angiogenesis [36].

Cellular binding assay is valuable for the analysis of the first step of inflammation in vitro [37, 38]. The attachment of mononuclear cells to the endothelium is essential in the initiation of atherosclerotic and inflammatory lesions, and it is well known that cell adhesion molecules play a key role in the development of inflammation and atherosclerosis [39]. TNFα-stimulated MAECs displayed cellular binding ability with WEHI-3B cells. Regarding the molecules that mediate these adhesions, various multiple adhesion molecules have been identified on activated ECs, including endothelial-leukocyte adhesion molecule-1 (E-selectin), VCAM-1, and ICAM-1. It was also demonstrated that VCAM-1 was expressed on MAECs activated by TNFα (fig. 5a). In addition, VLA-4, a ligand of VCAM-1, was expressed on WEHI-3B cells. These results demonstrated that VCAM-1 and VLA-4 contribute to the cellular binding activity of MAECs and WEHI-3B. In this manner, using MAECs, the interaction between cell adhesion molecules can be studied in detail.

Low-level NO production and a lower expression of eNOS in MAECs compared to HUVECs may result from the multiple passages of this cell line. Actually, Matsushita et al. [40] reported that eNOS activity was reduced in senescent human ECs, and shear stress induced greater eNOS expression and activity. From these results, although MAECs retained the endothelial characteristics regarding eNOS expression, the analysis of eNOS activity should be considered in various conditions, and MAECs may not be the ideal model for the study of NO and ECs.

p53 is a tumor suppressor protein that plays an important role in the cell cycle and cell growth. p53 protein deficiency causes mice to develop spontaneous tumors, and loss of p53 function results in genomic instability. Although many kinds of cell lines have been established from p53-deficient mice, in some cell lines genomic instability, accelerated growth, malignant transformation and some phenotypic changes were shown [17, 18, 41]. In this paper, our results showed that MAECs expressed vWf, whose production is often lost in transformed or malignant ECs in angiosarcomas [10, 28]. Therefore, we consider that MAECs are an established cell line which may not have obtained malignant transformation. However, further investigation will be needed regarding malignancy.

In conclusion, we propose that our EC line MAEC, which retains endothelial functions such as cellular binding activity and tube formation activity, could contribute significantly to the future study of EC biology. This cell line is freely available for the academic research community with a material transfer agreement.

Acknowledgments

This work was partially supported by grants-in-aid for scientific research from the Ministry of Education, Culture, Sports, Science and Technology of Japan. The authors gratefully thank Roger E. Morgan for helpful comments and critical reading of the manuscript, and Judith Nishino for helpful discussions during the preparation of this manuscript. The Sjögren's Syndrome Project of Keio University was supported by Kowa Co., Ltd.

References

1 Carmeliet P: Angiogenesis in health and disease. Nat Med 2003;9:653–660.
2 Jaffe EA, Nachman RL, Becker CG, Minick CR: Culture of human endothelial cells derived from umbilical veins. Identification by morphologic and immunologic criteria. J Clin Invest 1973;52:2745–2756.
3 Liu JJ, Huang TS, Cheng WF, Lu FJ: Baicalein and baicalin are potent inhibitors of angiogenesis: inhibition of endothelial cell proliferation, migration and differentiation. Int J Cancer 2003;106:559–565.
4 Chen HH, Zhou HJ, Fang X: Inhibition of human cancer cell line growth and human umbilical vein endothelial cell angiogenesis by artemisin in derivatives in vitro. Pharmacol Res 2003;48:231–236.
5 Dong QG, Bernasconi S, Lostaglio S, De Calmanovici RW, Martin-Padura I, Breviario F, Garlanda C, Ramponi S, Mantovani A, Vecchi A: A general strategy for isolation of endothelial cells from murine tissues. Characterization of two endothelial cell lines from the murine lung and subcutaneous sponge implants. Arterioscler Thromb Vasc Biol 1997;17:1599–1604.
6 Toyama-Sorimachi N, Miyake K, Miyasaka M: Activation of CD44 induces ICAM-1/LFA-1-independent, Ca^{2+}, Mg^{2+}-independent adhesion pathway in lymphocyte-endothelial cell interaction. Eur J Immunol 1993;23:439–446.
7 Kanda S, Landgren E, Ljungstrom M, Claesson-Welsh L: Fibroblast growth factor receptor 1-induced differentiation of endothelial cell line established from tsA58 large T transgenic mice. Cell Growth Differ 1996;7:383–395.
8 Lidington EA, Rao RM, Marelli-Berg FM, Jat PS, Haskard DO, Mason JC: Conditional immortalization of growth factor-responsive cardiac endothelial cells from H-2K(b)-tsA58 mice. Am J Physiol Cell Physiol 2002;282:C67–C74.
9 Harder R, Uhlig H, Kashan A, Schutt B, Duijvestijn A, Butcher EC, Thiele HG, Hamann A: Dissection of murine lymphocyte-endothelial cell interaction mechanisms by SV-40-transformed mouse endothelial cell lines: novel mechanisms mediating basal binding, and alpha 4-integrin-dependent cytokine-induced adhesion. Exp Cell Res 1991;197:259–267.
10 Masuzawa M, Fujimura T, Hamada Y, Fujita Y, Hara H, Nishiyama S, Katsuoka K, Tamauchi H, Sakurai Y: Establishment of a human hemangiosarcoma cell line (ISO-HAS). Int J Cancer 1999;81:305–308.
11 Lidington EA, Moyes DL, McCormack AM, Rose ML: A comparison of primary endothelial cells and endothelial cell lines for studies of immune interactions. Transpl Immunol 1999;7:239–246.
12 Arbiser JL, Larsson H, Claesson-Welsh L, Bai X, LaMontagne K, Weiss SW, Soker S, Flynn E, Brown LF: Overexpression of VEGF 121 in immortalized endothelial cells causes conversion to slowly growing angiosarcoma and high level expression of the VEGF receptors VEGFR-1 and VEGFR-2 in vivo. Am J Pathol 2000;156:1469–1476.
13 Tsukada T, Tomooka Y, Takai S, Ueda Y, Nishikawa S, Yagi T, Tokunaga T, Takeda N, Suda Y, Abe S, et al: Enhanced proliferative potential in culture of cells from p53-deficient mice. Oncogene 1993;8:3313–3322.
14 Nakayama T, Kanoe H, Sasaki MS, Aizawa S, Nakamura T, Toguchida J: Establishment of an osteoblast-like cell line, MMC2, from p53-deficient mice. Bone 1997;21:313–319.
15 Hasegawa S, Yamada K, Inoue H, Azuma N, Suzuki M, Matsuoka T: Establishment of pulmonary alveolar type II cell line from p53-deficient mice. Lung 2001;179:21–29.
16 Hanazono M, Nakagawa E, Aizawa S, Tomooka Y: Establishment of prostatic cell line 'Pro9ad' from a p53-deficient mouse. Prostate 1998;36:102–109.
17 Minakawa M, Sugimoto T, Aizawa S, Tomooka Y: Cerebellar cell lines established from a p53-deficient adult mouse. Brain Res 1998;813:172–176.
18 Yahanda AM, Bruner JM, Donehower LA, Morrison RS: Astrocytes derived from p53-deficient mice provide a multistep in vitro model for development of malignant gliomas. Mol Cell Biol 1995;15:4249–4259.
19 Sevignani C, Wlodarski P, Kirillova J, Mercer WE, Danielson KG, Iozzo RV, Calabretta B: Tumorigenic conversion of p53-deficient colon epithelial cells by an activated Ki-ras gene. J Clin Invest 1998;101:1572–1580.
20 Tanaka K, Sato M, Tomita Y, Ichihara A: Biochemical studies on liver functions in primary cultured hepatocytes of adult rats. I. Hormonal effects on cell viability and protein synthesis. J Biochem (Tokyo) 1978;84:937–946.
21 Weibel ER, Palade GE: New cytoplasmic components in arterial endothelia. J Cell Biol 1964;23:101–112.
22 Staunton DE, Dustin ML, Springer TA: Functional cloning of ICAM-2, a cell adhesion ligand for LFA-1 homologous to ICAM-1. Nature 1989;339:61–64.
23 Yamaguchi TP, Dumont DJ, Conlon RA, Breitman ML, Rossant J: flk-1, an flt-related receptor tyrosine kinase is an early marker for endothelial cell precursors. Development 1993;118:489–498.
24 Lynch DC, Zimmerman TS, Collins CJ, Brown M, Morin MJ, Ling EH, Livingston DM: Molecular cloning of cDNA for human von Willebrand factor: authentication by a new method. Cell 1985;41:49–56.
25 Carmeliet P, Lampugnani MG, Moons L, Breviario F, Compernolle V, Bono F, Balconi G, Spagnuolo R, Oostuyse B, Dewerchin M, Zanetti A, Angellilo A, Mattot V, Nuyens D, Lutgens E, Clotman F, de Ruiter MC, Gittenberger-de Groot A, Poelmann R, Lupu F, Herbert JM, Collen D, Dejana E: Targeted deficiency or cytosolic truncation of the VE-cadherin gene in mice impairs VEGF-mediated endothelial survival and angiogenesis. Cell 1999;98:147–157.
26 Chen CS, Toda KI, Maruguchi Y, Matsuyoshi N, Horiguchi Y, Imamura S: Establishment and characterization of a novel in vitro angiogenesis model using a microvascular endothelial cell line, F-2C, cultured in chemically defined medium. In Vitro Cell Dev Biol Anim 1997;33:796–802.
27 Sato N, Sato T, Takahashi S, Kikuchi K: Establishment of murine endothelial cell lines that develop angiosarcomas in vivo: brief demonstration of a proposed animal model for Kaposi's sarcoma. Cancer Res 1986;46:362–366.
28 Toda K, Tsujioka K, Maruguchi Y, Ishii K, Miyachi Y, Kuribayashi K, Imamura S: Establishment and characterization of a tumorigenic murine vascular endothelial cell line (F-2). Cancer Res 1990;50:5526–5530.

29 Mizuno R, Yokoyama Y, Ono N, Ikomi F, Ohhashi T: Establishment of rat lymphatic endothelial cell line. Microcirculation 2003; 10:127–131.
30 Su X, Sorenson CM, Sheibani N: Isolation and characterization of murine retinal endothelial cells. Mol Vis 2003;9:171–178.
31 Voyta JC, Via DP, Butterfield CE, Zetter BR: Identification and isolation of endothelial cells based on their increased uptake of acetylated-low density lipoprotein. J Cell Biol 1984;99:2034–2040.
32 Hirashima M, Kataoka H, Nishikawa S, Matsuyoshi N: Maturation of embryonic stem cells into endothelial cells in an in vitro model of vasculogenesis. Blood 1999;93:1253–1263.
33 Eichmann A, Corbel C, Nataf V, Vaigot P, Breant C, Le Douarin NM: Ligand-dependent development of the endothelial and hemopoietic lineages from embryonic mesodermal cells expressing vascular endothelial growth factor receptor 2. Proc Natl Acad Sci USA 1997;94:5141–5146.
34 Drake CJ, Fleming PA: Vasculogenesis in the day 6.5 to 9.5 mouse embryo. Blood 2000;95: 1671–1679.
35 Davis S, Aldrich TH, Jones PF, Acheson A, Compton DL, Jain V, Ryan TE, Bruno J, Radziejewski C, Maisonpierre PC, Yancopoulos GD: Isolation of angiopoietin-1, a ligand for the TIE2 receptor, by secretion-trap expression cloning. Cell 1996;87:1161–1169.
36 Su JD, Mayo LD, Donner DB, Durden DL: PTEN and phosphatidylinositol 3′-kinase inhibitors up-regulate p53 and block tumor-induced angiogenesis: evidence for an effect on the tumor and endothelial compartment. Cancer Res 2003;63:3585–3592.
37 Umetani M, Nakao H, Doi T, Iwasaki A, Ohtaka M, Nagoya T, Mataki C, Hamakubo T, Kodama T: A novel cell adhesion inhibitor, K-7174, reduces the endothelial VCAM-1 induction by inflammatory cytokines, acting through the regulation of GATA. Biochem Biophys Res Commun 2000;272:370–374.
38 Kaneko M, Hayashi J, Saito I, Miyasaka N: Probucol downregulates E-selectin expression on cultured human vascular endothelial cells. Arterioscler Thromb Vasc Biol 1996; 16:1047–1051.
39 Cybulsky MI, Gimbrone MA Jr: Endothelial expression of a mononuclear leukocyte adhesion molecule during atherogenesis. Science 1991;251:788–791.
40 Matsushita H, Chang E, Glassford AJ, Cooke JP, Chiu CP, Tsao PS: eNOS activity is reduced in senescent human endothelial cells: preservation by hTERT immortalization. Circ Res 2001;89:793–798.
41 Ohmi K, Masuda T, Yamaguchi H, Sakurai T, Kudo Y, Katsuki M, Nonomura Y: A novel aortic smooth muscle cell line obtained from p53 knock out mice expresses several differentiation characteristics. Biochem Biophys Res Commun 1997;238:154–158.

Clinical and Experimental Immunology | ORIGINAL ARTICLE | doi:10.1111/j.1365-2249.2007.03448.x

Amelioration of lacrimal gland inflammation by oral administration of K-13182 in Sjögren's syndrome model mice

T. Nishiyama,*†‡ K. Mishima,* K. Obara,* H. Inoue,* T. Doi,‡ S. Kondo,‡ M. Saka,‡ Y. Tabunoki,‡ Y. Hattori,‡ T. Kodama,§ K. Tsubota¶ and I. Saito*

*Department of Pathology, Tsurumi University School of Dental Medicine, Yokohama, Japan, †Sjögren's Syndrome Project, Shinanomachi Research Park, Keio University, Tokyo, Japan, ‡Tokyo New Drug Research Laboratories II, Pharmaceutical Division, Kowa Co. Ltd, Tokyo, Japan, §Laboratory for Systems Biology and Medicine, Research Center for Advanced Science and Technology, Graduate School of Medicine, University of Tokyo, Tokyo, Japan, and ¶Department of Ophthalmology, School of Medicine, Keio University, Tokyo, Japan

Accepted for publication 29 May 2007
Correspondence: Ichiro Saito, Department of Pathology, Tsurumi University School of Dental Medicine, 2-1-3 Tsurumi, Tsurumi-ku, Yokohama, 230–8501, Japan.
E-mail: saito-i@tsurumi-u.ac.jp

Summary

Regulation of the adhesion of mononuclear cells to endothelial cells is considered to be a critical step for the treatment of inflammatory diseases, including autoimmune diseases. K-13182 was identified as a novel inhibitor for these adhesions. K-13182 inhibited the expression of vascular cell adhesion molecule-1 (VCAM-1, CD106) on human umbilical vein endothelial cells (HUVECs) and on mouse vascular endothelial cell line (MAECs) induced by tumour necrosis factor (TNF)-α. K-13182 also inhibited the adhesion of mononuclear cells to these HUVECs and MAECs, indicating that K-13182 suppressed these adhesions mediated by cellular adhesion molecules including VCAM-1. To evaluate the therapeutic effect in autoimmune disease model mice, K-13182 was orally administered to non-obese diabetic (NOD) mice as Sjögren's syndrome (SS) model mice. Severe destructive inflammatory lesions were observed in the lacrimal glands of vehicle-treated control mice; however, 8-week administration of K-13182 inhibited the mononuclear cell infiltration into the inflammatory lesions of the lacrimal glands. In K-13182-treated mice, the decrease in tear secretion was also prevented compared to the control mice. In addition, the apoptosis and the expression of FasL (CD178), perforin, and granzyme A was suppressed in the lacrimal glands of K-13182-treated mice. Therefore, K-13182 demonstrated the possibility of therapeutic efficacy for the inflammatory region of autoimmune disease model mice. These data reveal that VCAM-1 is a promising target molecule for the treatment of autoimmune diseases as a therapeutic strategy and that K-13182 has the potential as a new anti-inflammatory drug for SS.

Keywords: autoimmune disease, endothelial cells, lacrimal gland, NOD mouse, VCAM-1

Introduction

Sjögren's syndrome (SS) is an organ-specific autoimmune disorder characterized by lymphocytic infiltration and progressive loss of exocrine glands resulting in symptoms of dry mouth and dry eye due to insufficient secretion, and systemic production of autoantibodies to the ribonucleoprotein [1]. Although a large number of studies have been conducted [2–5], the mechanism of the destruction of the exocrine glands is still unclear.

In the first stage of inflammatory diseases, leucocytes migrate from the circulation into the sites in which inflammation manifests. Leucocyte adherence to the blood vessel wall through cell adhesion molecules is the important step for leucocyte migration [6]. When activated by inflammatory cytokines, endothelial cells express adhesion molecules such as vascular cell adhesion molecule-1 (VCAM-1), intercellular adhesion molecule-1 (ICAM-1, CD54) and E-selectin (CD62E). VCAM-1 is a cell surface glycoprotein which belongs to the immunoglobulin superfamily, and is adhesive to certain blood leucocytes and tumour cells that bear α4 integrins. In the vascular system, VCAM-1 is expressed on activated endothelial cells, smooth muscle cells and fibroblasts in a variety of pathological conditions, including atherosclerosis and inflammation [7–9]. These former studies indicate that endothelial/lymphocyte adhesion involving VCAM-1/VLA-4 (CD49d/CD29) control the migration of lymphocytes into the inflamed lesion. These cell adhesion molecules offer potential therapeutic targets to block the development of inflammation and tissue destruction.

In SS, it has been reported that the expression of cell adhesion molecules on vascular endothelial cells, such as ICAM-1 and VCAM-1, increased in the salivary and lacrimal glands [10]. In addition, these adhesion molecules play predominant roles in controlling T cell recruitment into these tissues and in the regulation of inflammation [11].

In this study, we identified the newly synthesized, low molecular weight compound K-13182, which inhibited the VCAM-1 expression on human umbilical vein endothelial cells (HUVECs), mouse aortic vascular endothelial cell lines (MAECs) and inhibited cellular adhesion between HUVECs and U-937 human monocytic cell lines. The purpose of this study is to evaluate the therapeutic effect of K-13182 and to clarify the mechanism in detail in SS model mice.

Materials and methods

Cell cultures

HUVECs were purchased from Clontech (Palo Alto, CA, USA), and cultured in EGM-2 medium (Clontech). Three or four time-passaged cells were used for the experiments. U-937 was obtained from American Type Culture Collection (Manassa, VA, USA) and maintained in RPMI-1640 medium containing 10% fetal calf serum (FCS) (Invitrogen, Carlsbad, CA, USA). Murine myeloid leukaemia cell line, WEHI-3, was obtained from Riken Cell Bank (Ibaraki, Japan) and maintained in RPMI-1640 medium containing 10% FCS and 2-mercaptoethanol. MAECs were isolated and established from p53-deficient mice in our previous study [12].The cells were maintained in M199 (Sigma, St Louis, MO, USA) supplemented with 5% FCS, 10 U/ml heparin sodium (Shimizu Pharmaceutical, Shizuoka, Japan), 100 U/ml penicillin (Invitrogen) and 100 μg/ml streptomycin (Invitrogen).

Expression of VCAM-1 on HUVECs and MAECs

The expression of VCAM-1 on MAECs and HUVECs was analysed with cell enzyme-linked immunosorbent assay (ELISA). MAECs and HUVECs (1×10^4) were seeded onto 96-well culture plates (Becton Dickinson, Franklin Lakes, NJ, USA). Confluent cultures of cells were stimulated with 10 ng/ml tumour necrosis factor (TNF)-α in the presence of various doses of K-13182. Non-specific binding was blocked by the sequential addition of 3% non-fat dry milk/phosphate-buffered saline (PBS) and 5% goat serum/PBS for 1 h. Anti-human VCAM-1 (4B2, Genzyme Corporation, Cambridge, MA, USA) or anti-mouse VCAM-1 (MK2·7, American Type Culture Collection) and horseradish peroxidase (HRP)-conjugated goat anti-rat IgG antibody (R&D Systems, Minneapolis, MN, USA) were used as the first and second antibodies, respectively, followed by the addition of 3, 3′, 5, 5′-tetramethyl-benzidine (Moss Inc., Pasadena, MD, USA). The optical density (OD) of each well was determined by using a microplate reader (Bio-Rad Laboratories, Hercules, CA, USA) at 450 nm. The relative VCAM-1 expression was calculated using the following formula: (expression in the presence of K-13182 [OD]/expression in the absence of K-13182 [OD]) × 100. Data are expressed as mean ± standard deviation (s.d.) of three individual experiments.

Cellular adhesion assay

Cellular adhesion assay using HUVECs or MAECs and U-937 or WEHI-3 was performed as described in previous reports [12–15], with some modifications. Endothelial cells (HUVECs or MAECs, 1×10^4/well) were seeded into each well of 96-well culture plates. Confluent cultures of endothelial cells were stimulated by 30 ng/ml TNF-α and varying concentrations of K-13182 for 16 h at 37°C. U-937 or WEHI-3 cells were labelled with 10 μmol/l 2′,7′-bis(carboxyethyl)-5(6′) carboxyfluorescein tetraacetoxymethyl ester (PKH-2; Dojindo Laboratories, Kumamoto, Japan) for 1 h at 37°C in each medium for HUVECs and MAECs and then washed three times with serum-free medium. PKH-2-labelled cells (2×10^4) were added to each well and incubated with TNF-α-stimulated endothelial cells for 1 h. Cells that were not bound to endothelial cells were removed by inverting the plates for 30 min. Wells were subsequently washed once with serum-free M199, and the remaining cells were lysed with 1% Nonidet P-40 (Calbiochem, La Jolla, CA, USA). Fluorescence intensity in cell lysate was measured by using an automated microplate fluorometer (Perkin Elmer, Boston, MA, USA) at an excitation wavelength of 485 nm and an emission wavelength of 535 nm. The relative adhesion cells were calculated using the following formula: (adhesion in the presence of K-13182 [OD]/adhesion in the absence of K-13182 [OD]) × 100.

Reverse transcription–polymerase chain reaction (RT–PCR) assay

MAECs and HUVECs were stimulated with 10 ng/ml TNF-α in the presence of K-13182 for 4 h. Total RNA was extracted with TRIzol reagent (Life Technologies, Rockville, MD, USA), and cDNA was prepared from RNA with 50 pmol of random hexamer and 200 U of reverse transcriptase (Invitrogen); 0·5 μl of a 20-μl cDNA mixture was used for PCR with 5 pmol each of forward and reverse primers and 2·5 U of Ex *Taq* DNA polymerase (Takara Shuzo, Kyoto, Japan). The sequences of the specific sense and anti-sense oligonucleotide primer pairs were as follows: VCAM-1 (human), GGATAATGTTTGCAGCTTCTC and TTCAGTAAGTC TATCTCCAGC; VCAM-1 (mouse), CCCAAGGATCCA GAGATTCA and TAAGGTGAGGGTGGCATTTC; β-actin, CTCTTTGATGTCACGCACGATTTC and GTGGGCCGC TCTAGGCACCAA.

Samples were amplified through 25 or 30 cycles in a PCR Thermal Cycler (Applied Biosystems, Foster City, CA, USA).

Mice

Male non-obese diabetic (NOD) mice were purchased from Clea Japan, Inc. (Tokyo, Japan) and maintained under specific-pathogen-free conditions in the animal facilities of Kowa Tokyo New Drug Research Laboratories. All experimental protocols were approved by the animal welfare committees of Tsurumi University and Kowa Tokyo New Drug Research Laboratories.

Administration of K-13182

K-13182, dissolved in 0·5% hydroxypropyl methylcellulose, was administered orally into the mice at a dose of 30 mg/kg/day from 4 to 12 weeks of age (8 week of administration, $n = 12$) or from 4 to 16 weeks of age (12 week of administration, $n = 15$). For control mice, 0·5% hydroxypropyl methylcellulose was administered as vehicle for a period of 8 ($n = 12$) or 12 weeks ($n = 15$).

Measurement of tear secretion

Tear secretion was compared before and after administration of K-13182. We measured the tear secretion of NOD mice before administration (control mice: $n = 5$; K-13182-treated mice: $n = 5$) and 12 weeks after administration (control mice: $n = 10$; K-13182-treated mice: $n = 11$). Mice were anaesthetized intraperitoneally with a mixture of 36 mg/kg ketamine (Sigma) and 16 mg/kg xylazine (Sigma). The amount of secreted tears was determined by the length of the Schirmer strip soaked by tears (1 mm in width; Showa Yakuhin Kako, Tokyo) after insertion into the inner aspect of an eyelid every 5 min in a 20-min period.

Histological analysis

NOD mice were anaesthetized with diethyl ether (Wako Pure Chemical Industries, Osaka, Japan) and were killed. The lacrimal glands were then removed from K-13182-treated NOD mice ($n = 11$, 8 weeks of administration, $n = 15$, 12 weeks of administration) and control mice ($n = 11$, 8 weeks of administration, $n = 15$, 12 weeks of administration). Removed lacrimal glands were fixed with 4% paraformaldehyde and embedded in paraffin. The sections (4 μm) were prepared and stained with haematoxylin and eosin (H&E) [16] using the standard method. Histological grading of the inflammatory lesions in the lacrimal glands was performed according to the method proposed by White and Casarett [17]. The number of mononuclear cells on H&E-stained sections (three areas/section/animal) obtained from each animal was counted under a light microscope (× 400), and the mean value was calculated for each animal.

*Taq*Man RT–PCR

Lacrimal glands were removed from NOD mice as mentioned above. Total RNA were obtained from the lacrimal glands of K-13182-treated mice or control mice. Reverse transcription was performed using a GeneAmp RNA PCR kit (Applied Biosystems). *Taq*Man–PCR was also performed according to the manufacturer's instructions (Applied Biosystems). Oligonucleotide primers and probes are described in Table 1. Sequence specific amplification was detected with an increased fluorescent signal of reporter dye 6-carboxy fluorescein (FAM) during the following amplification cycles: 1 cycle at 50°C for 2 min, 1 cycle at 95°C for 10 min and 40 cycles each at 95°C for 15 s and 60°C for 1 min. Gene-specific mRNA was normalized subsequently to rRNA. Primers and probes for rRNA were purchased from Applied Biosystems.

TUNEL assay

Lacrimal glands were removed from NOD mice, as mentioned above, and were embedded in optimal cutting temperature compound (OCT; Sakura Finetechnical, Tokyo, Japan) and frozen in liquid nitrogen. Cryostat sections (5 μm) were made, and apoptotic cells were detected in sections by terminal deoxynucleotidyl transferase-mediated dUTP nick end labelling (TUNEL) assay using the *in situ* apoptosis *in situ* detection kit (Wako Pure Chemical Industries), according to the manufacturer's instructions. The percentage of TUNEL-positive cells were counted under the light microscope (× 400) in three fields per one section (TUNEL index), and expressed as mean percentage ± s.d. in four (control mice) or three (K-13182-treated mice) sections.

Table 1. Primers and probes used for reverse transcription–polymerase chain reaction (RT–PCR) analysis.

mRNA	Sequences
VCAM-1	
Forward primer	ACAAGTCTACATCTCTCCCAGGAATAC
Reverse primer	CACAGCACCACCCTCTTGAA
Probe	CTGTACATCCCTCCACAAG
FasL	
Forward primer	TCAGCTCTTCCACCTGCAGAA
Reverse primer	TACTTTAAGGCTTTGGTTGGTGAA
Probe	AACTGGCAGAACTCCGT
Perforin	
Forward primer	GCAGGTCAGGCCAGCATAA
Reverse primer	ACCTTTGAATCCTGGCACTCA
Probe	AGTAGCCATGATTCATGCC
Granzyme A	
Forward primer	GGTGGAAAGGACTCCTGCAA
Reverse primer	GCCTCGCAAAATACCATCACA
Probe	ATTCTGGCAGCCCTC

Results

K-13182 inhibited cellular adhesion and the expression of VCAM-1 in HUVECs

In our previous study, the expression of VCAM-1, ICAM-1 and E-selectin on the HUVECs in response to TNF-α was augmented markedly [15]. Among these cell adhesion molecules, K-13182 suppressed VCAM-1 expression in a dose-dependent manner ($P < 0.0001$ at 0·01, 0·03, 0·1, 0·3 and 1 μM compared to absence of K-13182, Dunnett's multiple comparisons, Fig. 1a). The observed half-maximal inhibitory concentration (IC_{50}) for VCAM-1 expression was 0·019 μM. To examine the specificity of K-13182, ICAM-1 expression was also analysed by cell ELISA. K-13182 (0·1–10 μM) did not show a suppressive effect on ICAM-1 expression (Fig. 1b). Suppression of VCAM-1 expression was also confirmed at the transcriptional level using RT–PCR, and 1 μM of K-13182 clearly inhibited the VCAM-1 mRNA expression that was induced by 10 ng/ml TNF-α (Fig. 1d). These results demonstrated that K-13182 specifically inhibited VCAM-1 expression.

We have established a mononuclear cell/endothelial cell adhesion assay system for the functional analysis of adhesion inhibitory compounds in a former report [15]. To assess whether K-13182 can function in lymphocytic cellular adhesion to activated HUVECs, this cellular adhesion assay was performed in the presence of K-13182. HUVECs were treated with TNF-α (10 ng/ml) for 4 h in the presence of

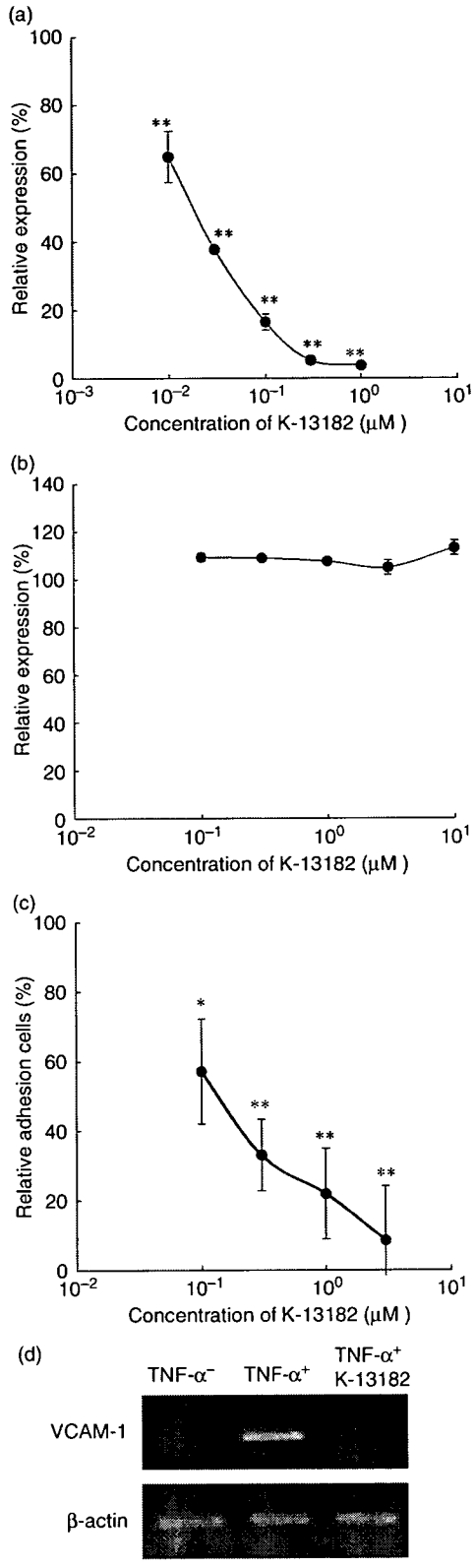

Fig. 1. The cell adhesion molecule expression and human mononuclear cell/endothelial cell adhesion. (a) Effects of K-13182 on vascular cell adhesion molecule-1 (VCAM-1) expression in human umbilical vein endothelial cells (HUVECs). HUVECs were stimulated with tumour necrosis factor (TNF)-α in the presence of K-13182 for 4 h. The expression of VCAM-1 was then investigated by cell enzyme-linked immunosorbent assay (ELISA). Data are expressed as percentage of control expression (without K-13182) and represented as mean ± s.d. of triplicate samples. Inhibitory concentration (IC_{50}) was 0·019 μM. Statistical analysis was made using Dunnett's multiple comparisons compared to absence of K-13182, $^{**}P < 0.001$. The results are the average of four separate experiments. (b) Effects of K-13182 on intercellular adhesion molecule-1 (ICAM-1) expression in HUVECs. ICAM-1 expression was not down-regulated by K-13182 in doses of 0–10 μM. (c) U-937/HUVECs adhesion assay. HUVECs were stimulated with TNF-α in the presence of K-13182 (0–3 μM) for 4 h. Adhesion of fluorescent-labelled U-937 cells were analysed by fluorescent spectrophotometer. IC_{50} was 0·14 μM. Data are expressed as percentage adhesion of cells added and represented as mean ± s.d. of triplicate samples. Statistical analysis was made using Dunnett's multiple comparisons compared to absence of K-13182, $^{*}P < 0.05$ and $^{**}P < 0.001$. (d) Effects of K-13182 on VCAM-1 mRNA expression in HUVECs. HUVECs were stimulated with 10 ng/ml TNF-α in the presence of 1 μM of K-13182 for 4 h. The expression of VCAM-1 was then investigated by reverse transcription–polymerase chain reaction (RT–PCR).